| | | | |
|---|---|---|---|
| **LAM**<br>**LOOM** | **Projet**<br>**FIRST** | REF**: LOOM.KD.SPIRE.2000.002-2**<br>Author **: Kjetil Dohlen** | PAGE : **1 / 1**<br>Date : **5 Dec. 2000** |

# FIRST SPIRE: Optical Error Budgets

**SPIRE-LAM-DOC-000446**

| | | | | |
|---|---|---|---|---|
| **RAL** | K.King | | | |
| | B.Swinyard | **X** | | |
| **CNES** | M.Joubert | | Y.Blanc | |
| **CEA-Sap** | Jean-Louis Auguères | | | |
| **LAS** | J.P.Baluteau | **X** | D. Ferrand | |
| | K.Dohlen | **X** | R. Malina | |
| | A.Origné | **X** | P.Dargent | **X** |
| | D.Pouliquen | **X** | | |
| | | | | |

**L**ABORATOIRE D'**A**STROPHYSIQUE DE **M**ARSEILLE - CNRS BP 8 13376 MARSEILLE Cedex 12 FRANCE
Tél : (33) +4 91 05 59 00 - Fax : (33) +4 91 05 69 59

# Updates

| Date | Indice | Remarks |
|---|---|---|
| 22 May 2000 | DRAFT | Creation of the document |
| 30 June 2000 | 1 | First release |
| 5 December 2000 | 2 | Exact sized photometer cold stop. Focus budget |
| | | |
| | | |
| | | |

# Reference documents

| # | Title | Author(s) | Reference | Date |
|---|---|---|---|---|
| 1 | FIRST alignment plan | | PT-PL-02220 | 9/5/96 |
| 2 | “Martin-Puplett interferometer: an analysis” | Lambert, Richards | Applied Optics **17**, 1595 (1978) | 1978 |
| 3 | Filters, Beam Splitters & Dichroics | P.A.R. Ade, C.E Tucker<br>M.J. Griffin, P.C.Hargrave | SPIRE Preliminary Design Review | 7-9 July 1999 |
| | | | | |
| | | | | |
| | | | | |

| | |
|---|---|
| Host system | Windows NT |
| Word processor | Microsoft Word 97 |
| File | ErrorBudgetsV2_01.DOC |
| Printed | 10/04/01 17:16 |

## 1. Scope

This document presents optical error budgets for SPIRE.

### *1.1. Table of contents*

**1. Scope ..... 5**

*1.1. Table of contents ..... 5*

**2. Introduction ..... 6**

*2.1. Baseline designs ..... 6*

**3. Photometer budgets ..... 7**

*3.1. Throughput ..... 7*

*3.2. Wavefront error ..... 9*

*3.3. Pupil alignment ..... 11*

**4. Spectrometer budgets ..... 14**

*4.1. Throughput ..... 14*

*4.2. Wavefront error ..... 16*

*4.3. Interferogram contrast ..... 17*

4.3.1. Optical design ..... 19
4.3.2. Interferometer alignment ..... 19
4.3.3. Beamsplitter balance ..... 23
4.3.4. Budget ..... 24

## 2. Introduction

Optical error budgets for the SPIRE instruments are presented. Throughput and wavefront error (Strehl ratio) budgets are presented for both photometer and spectrometer channels. Alignment tolerances are considered by way of a pupil alignment budget for the photometer and an interferogram contrast budget for the spectrometer.

### *2.1. Baseline designs*

Current baselines are BOLPHT153 for the photometer channel and BOLSP501B for the spectrometer channel. Schematic representations of the systems with symbolic names for each component are shown in Figure 1.

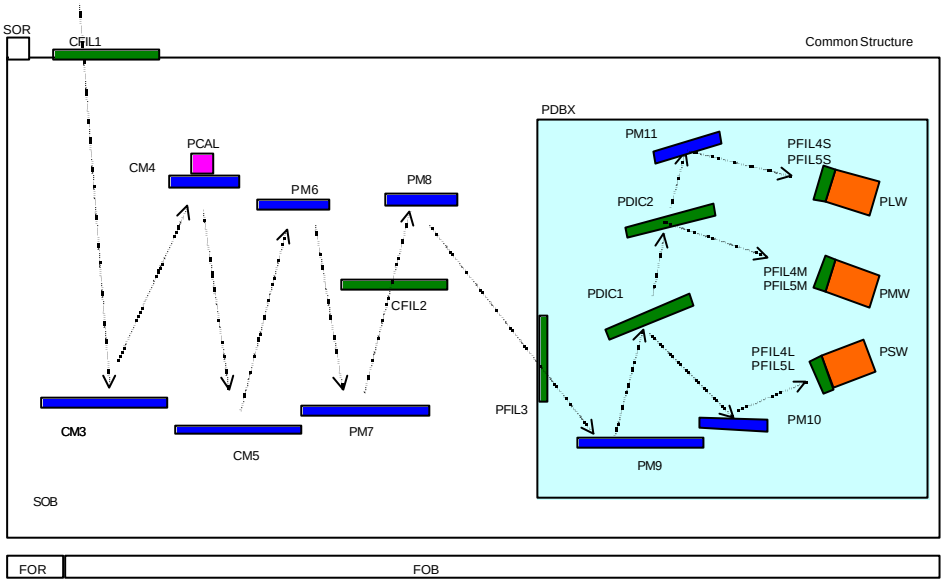


(a)

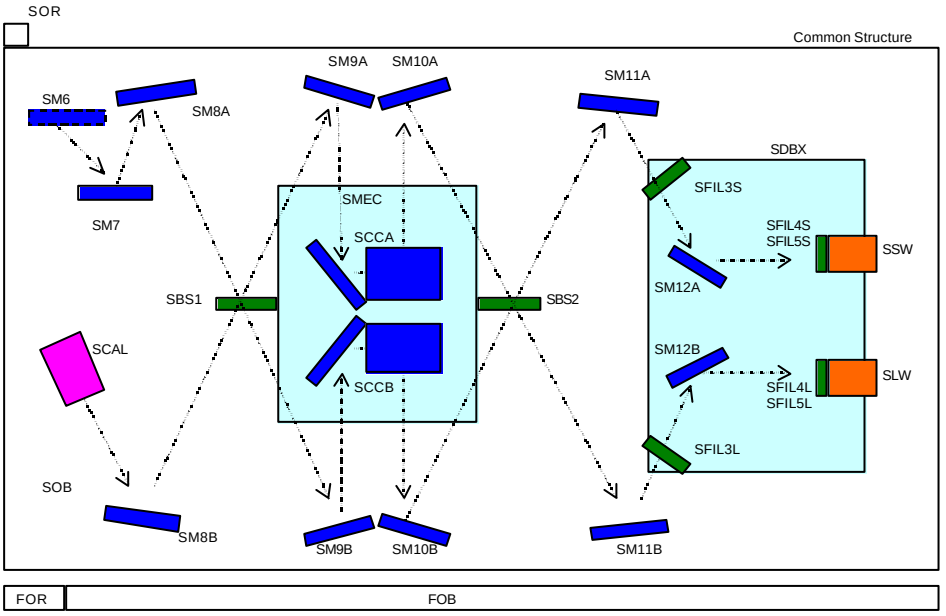


(b)

Figure 1. Schematic layout of the photometer channel (a) and spectrometer channel (b) of the SPIRE instrument.

## 3. Photometer budgets

### *3.1. Throughput*

Apart from filters and dichroics, major part of budget is due to sizing of cold stop. Undersizing was originally assumed, but it has been proven acceptable to use exact sizing of the cold stop. This means that the cold stop within the SPIRE instrument is given the dimensions of the geometrical image of the telescope pupil (M2). Due to variations in the pupil image for different points in the FOV (pupil aberrations) and instrument misalignments (see alignment budget, Sec. 3.3), the cold stop will not be exactly aligned with the telescope pupil, however, resulting in a loss of throughput. This loss has been estimated by considering the common area of displaced circles, see Figure below.

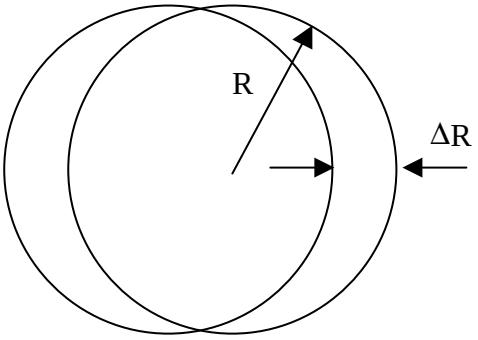


The transmission of the resulting system equals the fraction of the overlapping area ($A$) to the pupil area ($A_0$). With analogy to the calculation of optical MTF, this fraction may be given by the approximation:

$$\frac{A}{A_0} \approx 1 - \frac{2\Delta R}{p\,R} = 1 - 0.64\,\frac{\Delta R}{R},$$

where $\Delta R/R$ is the fractional displacement between the two circles.

Diffraction and baffling losses have been estimated to 20% (TBC).

Reflection efficiency assume a reflectivity of 99% per surface for 8 mirror surfaces.

Total filter and dichroic transmission has been assumed to be within the specified 40%

Current throughput budget (see Fig 2) is in accordance with the IRD requirement.

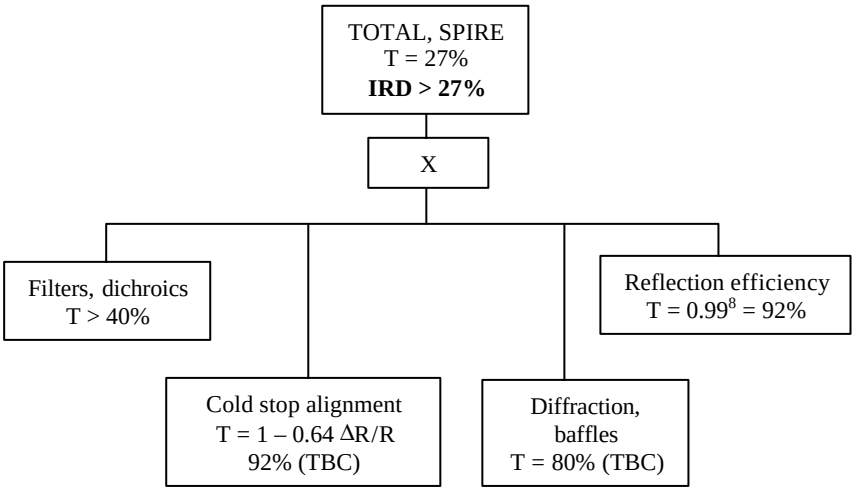


*Figure 2. Photometer throughput budget.*

*3.2. Wavefront error*

RMS wavefront errors (WFErms) are calculated at 250 µm. Total budget is obtained by RSS summing of individual budget values (Fig. 3). Strehl ratio is calculated by the Marechal approximation:

$$S \approx 1 - 4p^2 WFErms^2 = 1 - 4p^2 \sum_i WFErms_i^2$$

A WFErms of 2 µm per reflecting surface (ie, 1 µm rms measured on the surface itself) has been assumed for each of 9 surfaces (CM3 to PM9 plus 1 dicroic plus 1 fold mirror). Total WFErms is 2 µm $\sqrt{9}$ = 6 µm.

No contribution is assumed for transmissive components (filters and dichroics) since they are assumed to have zero optical thickness (TBC PA).

The mirror fabrication budget has been separated into two parts, considering surface shape and radius of curvature separately. A specification on radius of curvature of $\Delta R/R = 10^{-3}$ has been assumed for each surface. This may be translated into a wavefront error contribution per surface of

$$WFErms = \frac{h^2}{2\sqrt{3}R}\frac{\Delta R}{R}$$

where *h* is sub-pupil radius at the surface and *R* is nominal radius of curvature. Table 1 shows results of these calculations for each surface in the photometer optical train.

*Table 1. Defocus wavefront error due to $\Delta R/R = 10^{-3}$ precision on radius of curvature for each surface*

| Mirror | R | h | ΔR | WFErms |
|---|---|---|---|---|
| CM3 | 370 | 5.5 | 0.37 | 0.02 |
| CM5 | 300 | 18 | 0.3 | 0.31 |
| PM6 | 300 | 0.03 | 0.3 | 0.00 |
| PM7 | 330 | 19 | 0.33 | 0.32 |
| PM8 | 290 | 18 | 0.29 | 0.32 |
| PM9 | 350 | 35 | 0.35 | 1.01 |
| Total | | | | 1.15 |

The budget (Fig. 3) is well within the requirement. Note particularly that alignment errors as described in Sec. 3.3 contribute very little to the budget. The margin may be used to relax surface shape and/or focus requirements, but neither of these seem to be overly hard to reach.

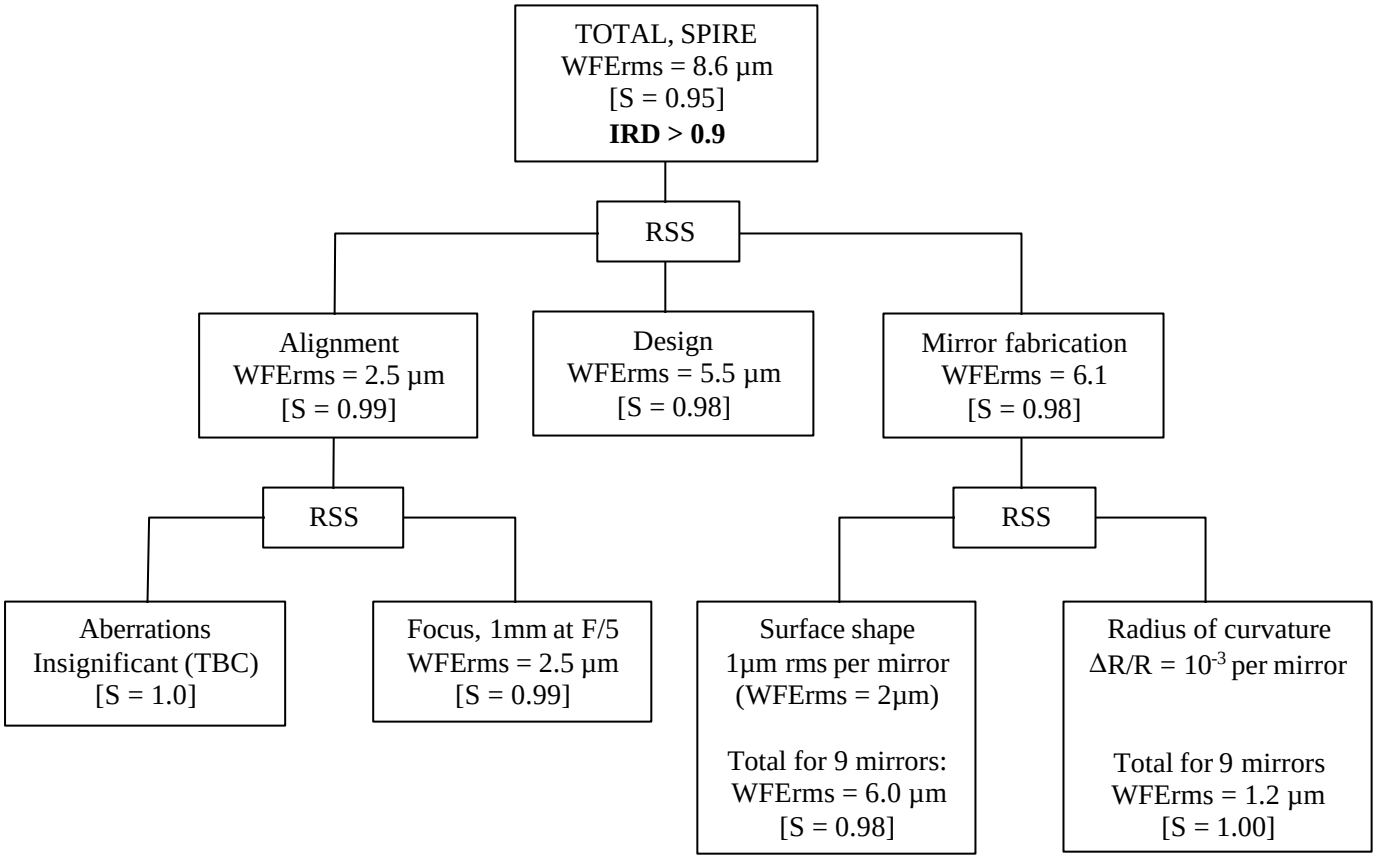


*Figure 3. Photometer wavefront error budget.*

### *3.3. Pupil alignment*

The pupil alignment budget (Fig. 4) is dimensioning for mechanical tolerances in the photometer case. There is no IRD on pupil alignment, but, as has been shown in the throughput budget (Fig. 2), it has a strong influence on instrument throughput.

The three major components concern design and alignment (FIRST and SPIRE), outlined in heavy lines in the figure. The design value quantifies the variation in pupil position for different points in the FOV for a perfectly aligned instrument, due to pupil aberrations. We believe that this value has been minimized for the optical concept chosen, and that a further reduction would require important complications of the optical design.

Degradation of pupil alignment due to mechanical misalignment consists of errors under ESA control (alignment between the FIRST telescope and its optical bench, FOB) and errors under SPIRE control. The latter is again broken down to errors due to the interface between theh FOB and the SPIRE optical bench (SOB), interfaces between SOB and mirrors, and interface between SOB and the cold-stop itself.

The ESA alignment plan [RD1] provides a total budget for absolute alignment between telescope and instrument of *"12¢ which corresponds to 16 mm lateral misalignment"*. Unfortunately, the document does not provide enough information to translate this into relative pupil alignment ($\Delta R/R$), and using data from the current telescope design (focal ratio F = 8.68, secondary diameter $D_{M2}$ = 308 mm), the two quoted numbers give different results. Calculated using the focal ratio and the angular tolerance:

$$\Delta R/R = 2\ F\ \delta\alpha = 6\%,$$

while using the M2 diameter and the linear tolerance:

$$\Delta R/R = 2\ \Delta R/D_{M2} = 10\%.$$

The former is assumed for the IID-B specification.

The budget shows a good balance between its three major components. The contribution from instrument alignment is the smallest, indicating that no great improvement can be expected from reducing the mechanical tolerance values.

Mechanical tolerances have been set to 0.1 mm decenter for each component along each direction x, y, z and 1arcmin tilt for each component around each axis. The effect of misalignments equal to these values for each component and each axis are obtained from a sensitivity analysis, summarized in Figure 5 (BolPhtRev05.mac, SpirePhotTol18.xls). Verification of the effect of random distributions of alignment errors is shown by the histogram plot of Figure 6 (SpirePhotTol20.xls).

Note that the components following the cold stop (PM9, folds, dichroics) have no influence on the CS alignment budget. Also, filters are not included since their thickness, and hence beam deviation, is negligible (TBC PA).

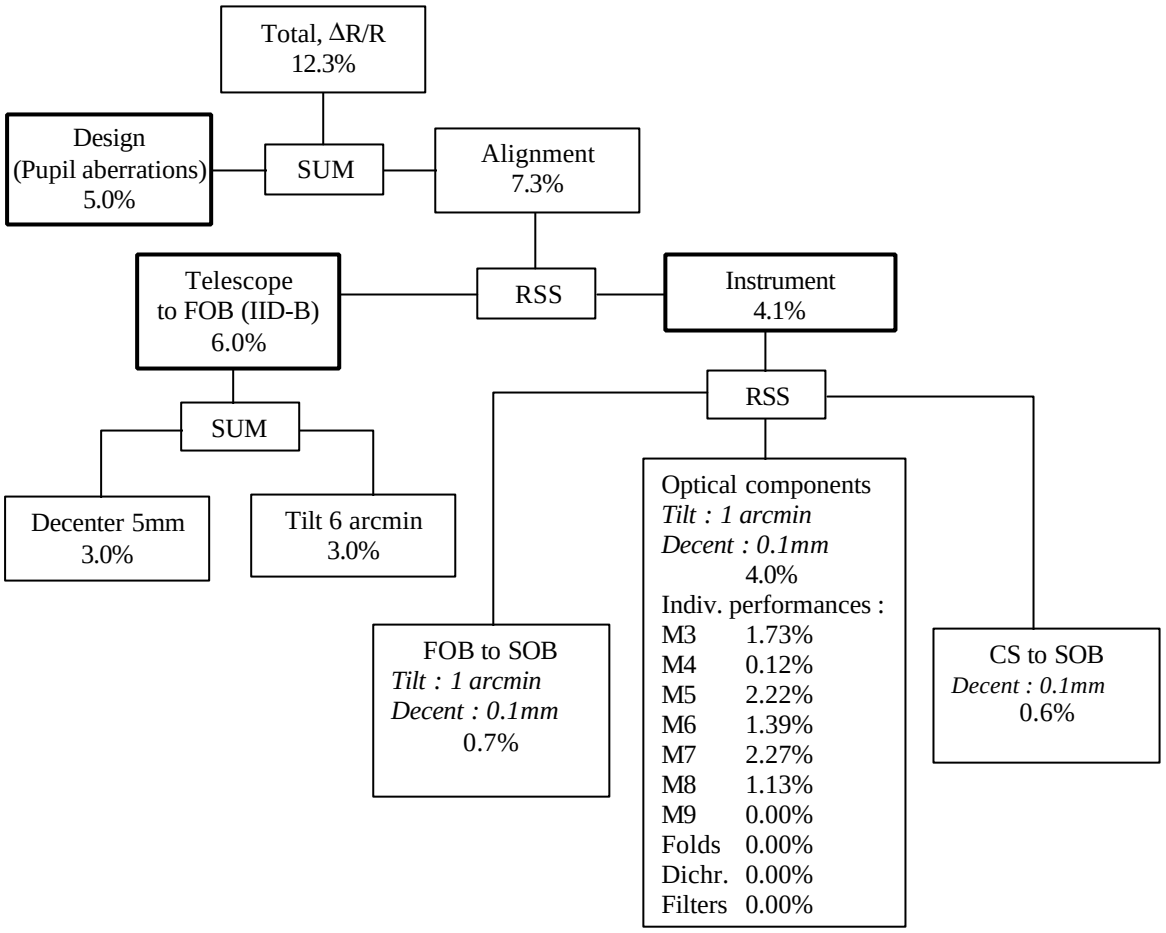


*Figure 4. Pupil alignment budget for the photometer. The heavy boxes indicate the tree major components of the budget: optical design (pupil aberrations) telescope alignment under ESA responsibility, and SPIRE alignment.*

*The SPIRE alignment budget assumes mounting accuracy of 0.1mm and 1arcmin for each interface: the SPIRE optical bench (SOB) mounted on the FIRST optical bench (FOB), each mirror in the optical train mounted on the S-bench, and the cold stop (CS) mounted on the SOB. These tolerances should in each case be distributed on the required intermediate interfaces. For example, the CS is mounted on the 2K box which is in turn mounted on the SOB.*

*The two top budget components, design and alignment, are summed because the pupil aberrations are deterministic. All other components are "root-sum-squared". As shown by Monte-Carlo simulation (Figure 6 below), assuming a uniform statistical distribution of errors within the tolerance bounds, this budget covers more than 90% percent of the real cases.*

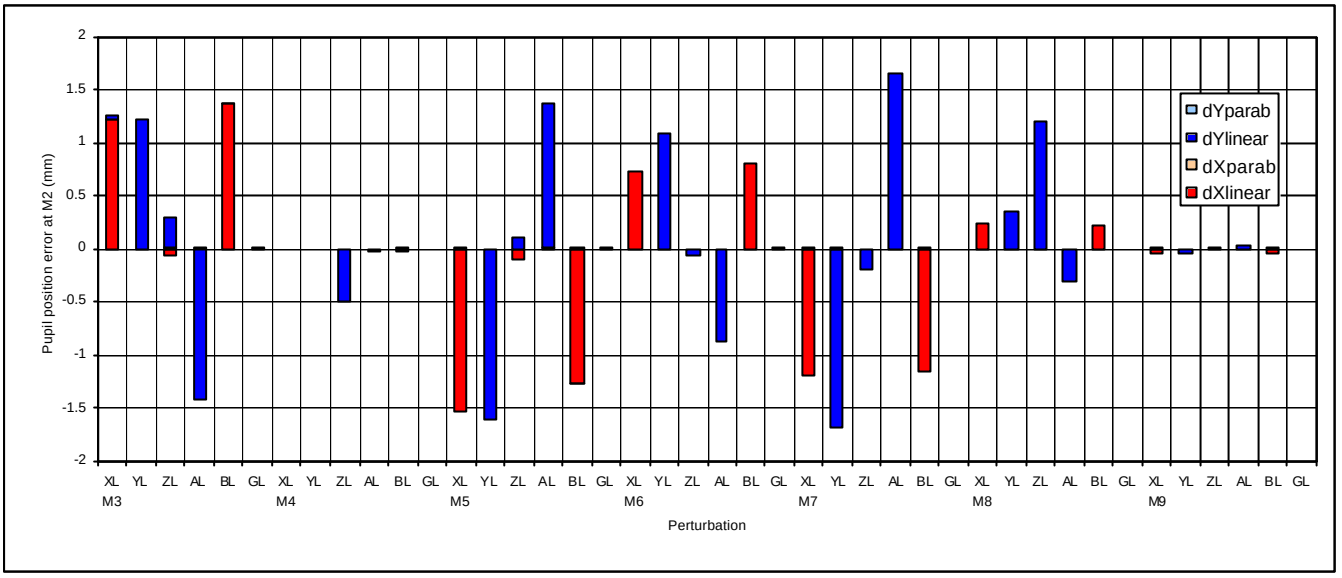


*Figure 5. Sensitivity of each photometer mirror to 0.1mm decenter tolerance (XL along x axis, YL along y axis, ZL along z axis) and to 1arcmin rotation tolerance (AL around x axis, BL around y axis, GL around z axis). Apart from M3 and M5, the z axis is perpendicular to each surface at its apex, the y axis is perpendicular to z in the plane of the system, the x axis is perpendicular to y and z. For M3 and M5, the z axis is shifted by 20mm so as to coincide approximately with the centre of gravity of the mirrors, and tilted so as to be perpendicular to the surface at that point.*

*Results are in mm measured at the M2. For an M2 radius of 150mm, an error DR = 1mm corresponds to a fractional pupil alignment error of DR/R = 0.67%. Red bars show displacements along the x direction, blue bars along the y direction. Light blue and light red correspond to non-linear sensitivity components: these are clearly insignificant.*

*Apart from M4 (conjugated with the pupil) and M9 (not involved in pupil imaging since after the cold stop), all mirrors have similar sensitivities. Errors due to GL tilts (azimuth rotation) are very small for all mirrors, the alignment budget is not dimensioning for these perturbations. A tolerance of about 0.5 degrees is probably acceptable to avoid vignetting.*

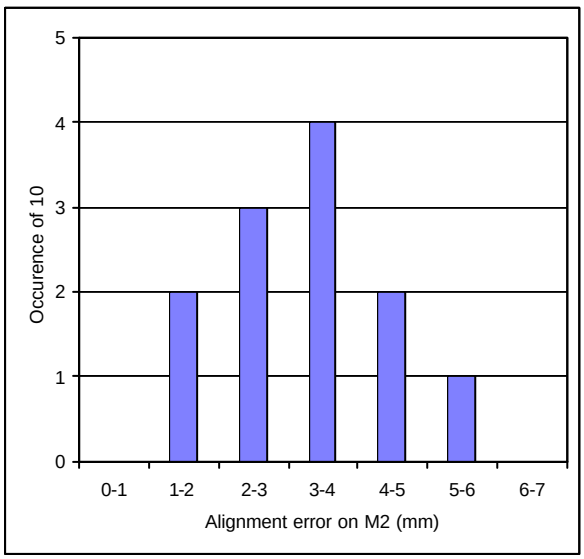


*Figure 6. Monte Carlo analysis with 10 randomly generated combinations of alignment errors. Each mirror has been given decenters and tilts up to ±0.1mm and ±1arcmin in each direction with an even statistical distribution. The resulting average error is 3.4mm (DR/R = 2.2%) and the 90% percentile is at 4.8mm (DR/R = 3.2%), i.e. less than the RSS assumption made in the error budget (Figure 3). This provides a "confidence margin". [The RSS assumption actually works with standard deviations. Since the standard deviation of an even distribution between ±a is s = a/Ö3, there is a factor Ö3 between the Monte-Carlo average and the RSS sum: 2.2% Ö3 = 3.8%, compared with 4.0% in the budget.]*

## 4. Spectrometer budgets

### *4.1. Throughput*

In the spectrometer case, the elimination of flux from M2 surrounds has been judged less of a problem, particularly because the spectrometer does not rely on chopping (signal is modulated by the FTS itself). We have therefore assumed an oversized (no-loss) cold stop. Losses due to diffraction and baffling are estimated to 20% (TBC). We have assumed 99% reflectivity of each of 13 mirror surface (CM3 to SM12 plus three CC surfaces) and a total filter and beamsplitter efficiency of 40%.

The throughput loss of 50% due to band-pass filtering is not included (cf BMS).

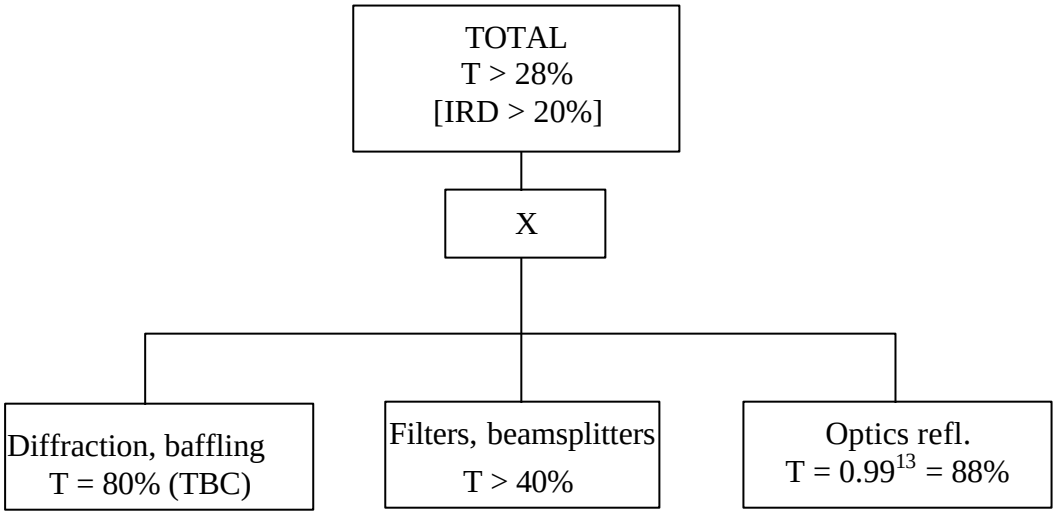


*Figure 7. Spectrometer throughput budget.*

*4.2. Wavefront error*

Wavefront error budget meets IRD with margin. See Sec. 3.2 for comments.

RMS surface error of 1 µm (2µm WFErms) is assumed for each of 15 reflecting surfaces (CM3 to SM12 plus 3 CC surfaces plus 2 BS surfaces). Transmissive components are not included since their thickness is negligible (TBC PA).

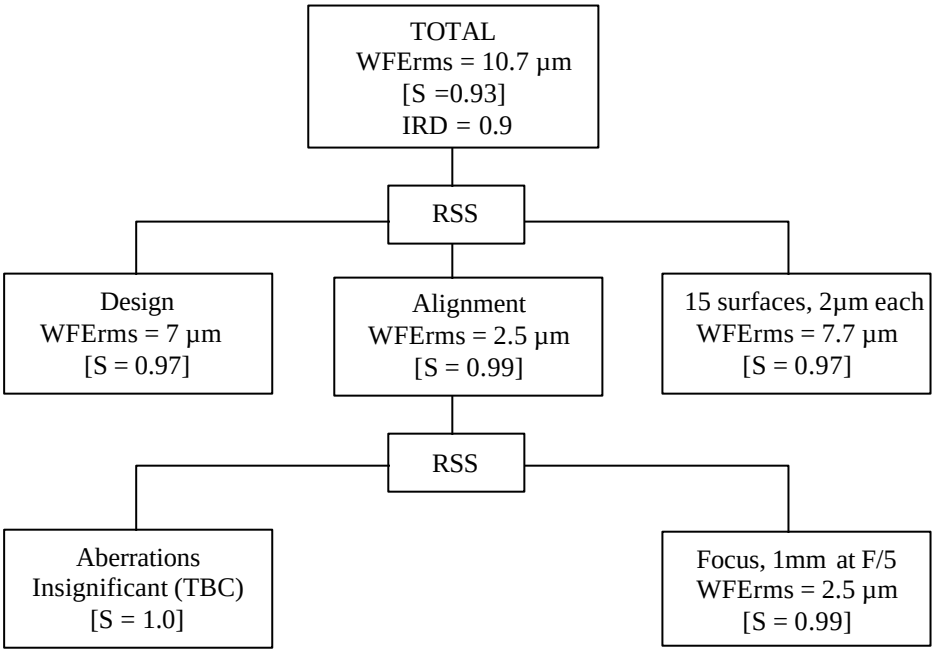


*Figure 8. Spectrometer wavefront budget.*

*4.3. Interferogram contrast*

Contrast is affected by tilt and shear between the interfering wavefronts and balance between beamsplitter R and T. Tilts and shears are discussed in the following, beamsplitter balance is discussed in sec. 4.3.3.

Interferogram contrast describes the efficiency with which the instrument renders the undulating interference intensity created by the FTS. It is defined for a monochromatic beam as:

$$k = \frac{I_{\max} - I_{\min}}{I_{\max} + I_{\min}} \tag{1}$$

where $I_{\max}$ and $I_{\min}$ are maximum (constructive) and minimum (destructive) interference intensities, respectively.

When OPD > 0, wavefronts from an off-axis object are sheared due to geometry, and may be tilted due to differential distortion. Misalignments of components within the interferometer also introduce tilt and shear.

When interfering wavefronts are tilted by angle $q$, the image on the detector is shifted by a displacement $D = qf$ where $f$ is the camera focal length. Using the van Cittert Zernike theorem, Lambert and Richards [RD2] calculate the resulting fringe contrast as:

$$k_T = 2J_1(u)/u \tag{2}$$

where $u = 2pD/(lF)$. Eq. (2) assumes an evenly illuminated aperture stop, it is therefore a conservative approximation for SPIRE since the Gaussian-mode beam tends to underilluminate the pupil. The actual contrast loss is therefore less than estimated from the above formula.

Applying Taylor expansion to eq. (2) provides an approximation valid for small perturbations:

$$k_T \approx 1 - u^2/8 = 1 - 0.79\Delta^2 \tag{3}$$

when $l$ = 250µm and $F$ = 5.

When wavefronts are sheared, the two interfering beams enter the focal plane at different angles, hence creating fringes across each detector. The detector integrates the fringe intensity, hence reduces the apparent interferogram contrast. It is easy to see that for a square detector with uniform response the contrast becomes zero when the fringe period is equal to the detector width. The contrast is in this case described by a sinc function and may be expressed as:

$$k_S = \sin(u)/u \tag{4}$$

where $u = pws/(Fld)$, $w$ is detector width, $s$ is pupil shear, and $d$ is pupil diameter. Assuming $w = 2Fl$, the argument simplifies to: $u = 2ps/d$. Again this is a conservative approximation of the actual case of horn detectors with Gaussian response and circular aperture.

Applying Taylor expansion to this formula gives:

$$k_S \approx 1 - u^2/6 = 1 - 0.011s^2 \tag{5}$$

when $d$ = 25mm. Note that (5) is independent of wavelength since horn size is scaled with the wavelength.

4.3.1. Optical design

Two sources of contrast loss due to optical design are identified:

*1) Shear for off-axis object.* An off-axis beam travelling through the interferometer at angle $\beta$ has a shear of:

$$s = OPD \sin\beta \approx OPD\ \beta$$

The angle $\beta$ for an object at the edge of the FOV is given by the Lagrange invariant as

$$\beta = FOV\ D/(2d)$$

where FOV is diameter of the sky field of view and D is the telescope entrance pupil diameter. Assuming FOV = 2.6′, D = 3300mm, d = 25mm, we get $\beta$ = 2.86°. At the nominal resolving power of 100, the maximum OPD is 12.5mm, hence pupil shear is s = 0.62mm. At maximum resolving power (1000), the shear is s = 6.2mm. Contrasts estimated by eq (5) are 99.6% and 64%, respectively.

*2) Tilt due to differential distortion.* Since there is powered optics within the interferometer and the OPD scanning causes a longitudinal displacement of the exit pupil, differential aberrations between the two interfering beams may occur. No significant difference in wavefront error has been detected, but a slight difference in distortion causes a shift of the image position (ie wavefront tilt) for off-axis objects. The shift increases linearly with OPD and reaches $\Delta$ = 0.04mm at R = 100 and $\Delta$ = 0.4mm at R = 1000. Contrasts estimated by eq. (3) are 99.8% and 88%, respectively.

4.3.2. Interferometer alignment

Contrary to optical design losses, alignment losses are independent of OPD and FOV. Tilts and decenters of each component within the interferometer in general introduce both tilts and shears to the interfering wavefronts. Table 1 gives wavefront tilts and shears produced by 0.1mm decenters and 1′ tilts of each component within the interferometer. The RSS of tilt and decenter values are calculated, and the total budgets estimated by multiplication with $\sqrt{}$(2N), where the $\sqrt{}$2 factor accounts for errors in both x and y directions, and N is the number of components in each case. The total budgets shows fringe contrast in brackets.

Clearly, the most critical components are the collimator and camera mirrors. Any significant reduction in alignment precision of these components will have important impacts on the alignment budget. Beamsplitter and corner cube alignments are far less critical. Tolerances may be relaxed in these cases, this may be particularly interesting for the internal alignment of the corner cubes.

In discussions with Guy Michel and Don Jennings, it became clear that they considered some adjustment capability highly desirable, at least for the qualification model, to allow optimizing cold IR operation. CIRS was originally designed without adjustments, but this was included later and proved useful during “debugging” of the qualification model. It is not clear how this could be realised in SPIRE, but it should be discussed. Don also suggests that the imaging capability of SPIRE may be utilised in the cold alignment check, eliminating the need for "cold fiddeling". TBT (=To be thought about :)

**Important note: The current budget concerns the scientific beam. Constraints due to mechanical or sensor concerns may in some cases be overriding.**

*Table 1. Wavefront tilts and shears due to 1¢ tilts and 0.1mm decenters*

| | 1¢ tilt | | 0.1mm decenter | | Total per comp, per dimension | | Nb of units | Total budgets (contrast) | |
|---|---|---|---|---|---|---|---|---|---|
| **Component** | **Tilt, D (mm)** | **Shear, s (mm)** | **Tilt, D (mm)** | **Shear, s (mm)** | **Tilt, D (mm)** | **Shear, s (mm)** | | **Tilt, D (mm)** | **Shear, s (mm)** |
| **Beamsplitter** | 0.023 | 0.087 | 0 | 0 | 0.023 | 0.087 | 2 | 0.046 (99.8%) | 0.174 (99.97%) |
| **Collimator** | 0.075 | 0.087 | 0.1 | 0.12 | 0.13 | 0.15 | 2 | 0.26 (95%) | 0.30 (99.9%) |
| **Camera** | 0.075 | 0.087 | 0.1 | 0.12 | 0.13 | 0.15 | 2 | 0.26 (95%) | 0.30 (99.9%) |
| **CC relative[1]** | 0 | 0 | 0 | 0.2 | 0 | 0.2 | 2 | 0 (100%) | 0.40 (99.8%) |
| **CC internal[2]** | 0.038 | 0 | NA | NA | 0.038 | 0 | 2 | 0.076 (99.5%) | 0 (100%) |
| **CC scan axis[3]** | 0 | 0 | 0 | 0 | 0 | 0 | 1 | 0 (100%) | 0 (100%) |
| **Total** | | | | | | | | **89.6%** | |

Notes:

1) Relative alignment between upper and lower CC vertices. Axial separation is not critical for contrast but should be kept below 1 mm.

2) Misalignments of the CC facets which cause 1′ beam deviation between input and output beams is assumed.

3) Fringe contrast is insensitive to tilts and decenters of perfectly mounted back-to-back corner cubes during the scan. Decenters give pupil movement however, so to avoid vignetting, the decenter should be less than 1 mm, say.

4.3.3. Beamsplitter balance

If interference is formed between two wavefronts of intensity $I_1$ and $I_2$, then the contrast of the interference fringes may be expressed as:

$$k = \frac{2\sqrt{I_1 I_2}}{I_1 + I_2}. \quad (6)$$

In a Mach-Zehnder, dual output configuration with two identical beamsplitters of reflectivity R and transmissivity T, the intensities $I_1$ and $I_2$ may be expressed in terms of R and T for each of the two outputs A and B:

$$I_{1A} = I_{2A} = RT, \quad (7)$$

$$I_{1B} = R^2 \quad \text{and} \quad I_{2B} = T^2. \quad (8)$$

By eq. (6) we therefore have:

$$k_A = 1,$$

$$k_B = 2RT/(R^2 + T^2).$$

The A output therefore has 100% contrast regardless of beamsplitter performance. Reading values of R and T off the curves presented by PA at the July 99 PDR [RD3], we find approximate contrast values for the B output, see Table 2. For the budget we have taken the worst-case contrast of 94%, occuring at 190 and 500 µm.

*Table 2. Approximate contrast for the B output.*

| $\lambda$ **(µm)** | **R (%)** | **T (%)** | **$k_B$ (%)** |
|---|---|---|---|
| 190 | 58 | 40 | 93.5 |
| 250 | 51.5 | 46 | 99.4 |
| 333 | 54.3 | 43.9 | 97.7 |
| 500 | 56 | 40 | 94.6 |
| 625 | 46 | 46 | 100 |
| 1000 | 26 | 67 | 67.5 |

4.3.4. Budget

Figure 9 shows the interferometer alignment budget. Nominal (R = 100) contrast values are shown and R = 1000 values are indicated in brackets. With a total budget of 84% for nominal resolving power, the required contrast of 80% is achieved with margin.

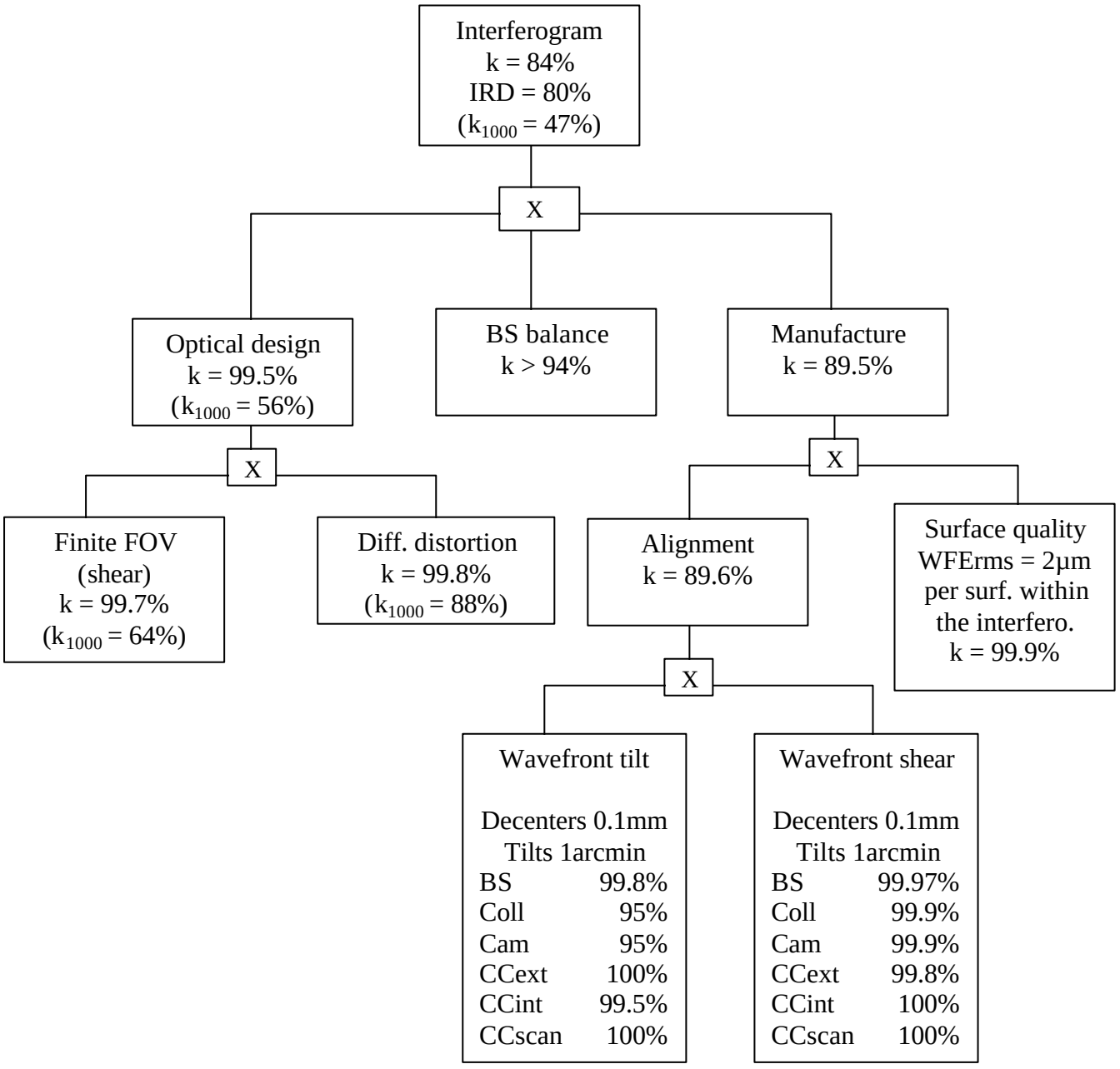


Figure 9. Interferometer alignment budget calculated at 250 µm. Nominal (R = 100) contrast values are shown and R = 1000 values are indicated in brackets.